The Journal of Chemical Physics

Characterization of charge carrier behavior in photocatalysis using transient absorption spectroscopy

Cite as: J. Chem. Phys. **152**, 194201 (2020); https://doi.org/10.1063/5.0008537
Submitted: 23 March 2020 . Accepted: 03 May 2020 . Published Online: 20 May 2020

Tina Jingyan Miao, and Junwang Tang

The Journal of Chemical Physics ARTICLE scitation.org/journal/jcp

Characterization of charge carrier behavior in photocatalysis using transient absorption spectroscopy

Cite as: J. Chem. Phys. 152, 194201 (2020); doi: 10.1063/5.0008537
Submitted: 23 March 2020 • Accepted: 3 May 2020 •
Published Online: 20 May 2020

Tina Jingyan Miao[1,2] and Junwang Tang[1,a)]

AFFILIATIONS

[1] Department of Chemical Engineering, University College London (UCL), WC1E 7JE London, United Kingdom
[2] Department of Chemistry, University College London (UCL), WC1H 0AJ London, United Kingdom

Note: This paper is part of the JCP Special Topic on Photocatalysis and Photoelectrochemistry.
[a)] **Author to whom correspondence should be addressed:** junwang.tang@ucl.ac.uk

ABSTRACT

Photocatalysis is a promising sustainable method to generate solar fuels for the future, as well as having other applications such as water/air purification. However, the performance of photocatalysts is often limited by poor charge carrier dynamics. To improve charge carrier dynamics, it is necessary to characterize and understand charge carrier behavior in photocatalytic systems. This critical review will present Transient Absorption Spectroscopy (TAS) as a useful technique for understanding the behavior of photoexcited charges in semiconductor photocatalysts. The role of TAS amongst other techniques for characterizing charge carrier behavior will be outlined. Basic principles behind TAS will be introduced, and interpretation of TAS spectra and kinetics will be discussed in the context of exemplar literature. It will be demonstrated that TAS is a powerful technique to obtain fundamental understanding of the behavior of photoexcited charges.

I. INTRODUCTION

There has been much research into solar-fuel generation through a variety of methods;[1–4] amongst these, photocatalysis is particularly promising due to the directness and pliability of this method. Briefly, the photocatalytic process is generally described as consisting of three steps: (1) photon absorption by a semiconductor photocatalyst resulting in the generation of excited charge carriers, (2) diffusion of excited charge carriers to surface reactive sites, and (3) interfacial charge transfer between the photocatalyst and surface chemical species, with the overall effect being catalysis of redox reactions. However, rather than proceeding to partake in redox reactions, photoexcited electrons and holes could, instead, recombine, which results in a loss of useful energy. Recombination is commonly identified as a key factor in limiting photocatalytic efficiency.[5–8] The rate of recombination determines the charge carrier lifetime [the average amount of time that elapses between the generation and annihilation (through recombination) of excited electrons/holes], which must necessarily be longer than the relevant reaction time scales to allow any significant amount of catalysis to occur. It may also be inferred that higher energy conversion efficiencies require longer charge carrier lifetimes, as the probability of an excited charge carrier partaking in redox catalysis increases relative to the probability of recombination. In addition, charge carrier lifetimes directly affect the diffusion length (here defined as the average distance traveled by an excited electron/hole between its generation and annihilation through recombination), which is a key factor to consider when rationally designing nanostructured photocatalysts.

For the continuous advancement of rationally designed photocatalysts, it is necessary to characterize and understand the dynamics of photoexcited charge carriers. A large repertoire of techniques exists for obtaining different information on various aspects of charge carrier dynamics; in essence, all these techniques involve sample excitation followed by monitoring of the time-dependent response of the system. In most techniques, the sample is excited

through illumination by photons with sufficient energy to bridge the bandgap. The time-dependent response of the system is then monitored through electrical measurements or by using an electromagnetic probe.

Techniques that use electrical measurements to monitor charge carrier behavior include Electrochemical Impedance Spectroscopy (EIS), Intensity Modulated Photovoltage Spectroscopy (IMVS), Intensity Modulated Photocurrent Spectroscopy (IMPS), and transient photocurrent/photovoltage (TPC/TPV). All of these techniques require some form of physical contact between the photocatalytic material and the measurement system, and most of these require the sample to be incorporated into an electrical circuit. This is straightforward if the material was designed as a photoelectrode; however, this is not true in many cases, and extra sample preparation steps are needed to obtain good electrical contact between the photocatalyst and the measurement system. By replacing electrical contacts with an electromagnetic probe, sample preparation can be greatly simplified in cases where good electrical contacts are difficult to achieve. In addition, the above-mentioned electrical techniques typically have time-resolution on the order of microseconds to seconds,[9–12] whereas techniques that employ an electromagnetic probe typically have time-resolutions on the order of femtoseconds to microseconds.[13–18]

There are a large range of techniques that use electromagnetic radiation to monitor ("probe") charge carrier behavior after photoexcitation and can be classified according to the nature of the electromagnetic probe or the type of interaction the probe has with the sample. Common interactions between the probe and the sample include absorption, scatter, and photoemission. Absorbance can be calculated by measuring either the transmitted or scattered/reflected probe, scatter can be elastic (i.e., diffuse/specular reflection) or inelastic (e.g., Raman), and photoemission occurs when high-energy ionizing probes (e.g., x-ray) are used. Regardless of the probe wavelength and the interaction type, these techniques are usually referred to as "pump–probe" techniques, as a measurement involves the pulsed excitation ("pump") of the sample followed by the monitoring of the relaxation of the excited sample using an electromagnetic probe.

Different regions of the electromagnetic spectrum are used to obtain different types of information, as summarized in Fig. 1 in the context of a semiconductor sample. Usually, probes in the microwave and far-IR [i.e., Terahertz (THz)] regions monitor free electrons (holes) in the conduction band (CB) [valence band (VB)]. As these are the dominant species giving rise to conductivity, the transient conductivity is usually reported for such measurements. For microwave probes, the measurement is usually referred to as Time-Resolved Microwave Conductivity (TRMC), whereas Terahertz (THz) measurements are usually called Time-Resolved Terahertz Spectroscopy (TRTS). Note here that TRTS is different from Terahertz Time-Domain Spectroscopy (THz-TDS), which is a static measurement technique.[19,20] As mid-IR is sensitive to molecular vibrations, probes in this region have been used to monitor vibrational changes in surface covalent chemical species[21,22] and molecular photocatalysts[23,24] though it has also been applied to monitor photoexcited charges in inorganic materials.[25–28] Along with mid-IR, near-IR and visible light are the most commonly used probes due to the relatively easy detection and generation of these wavelengths. Measurements that probe in the mid-IR region are usually referred to as Time-Resolved IR (TRIR), whereas measurements that probe in the visible/near-IR region are often referred to as Transient Absorption Spectroscopy (TAS), despite that any probe wavelength can be used to obtain a "transient absorption" (TA) signal. Probes in the extreme ultraviolet (XUV) and x-ray regions have also been recently used for the characterization of photocatalytic materials. Due to the element and oxidation state specificity of these probes, charge transfer between different species as a result of photoexcitation can be observed.[29–31] In addition to pump–probe techniques, photoluminescence (PL) is also shown in Fig. 1 because it is routinely used to characterize radiative recombination in photocatalysts.[32] Similarly, Time-resolved PL (TRPL) is often used to monitor rates of radiative recombination.[33,34] As external probe radiation is not used, TRPL is not considered a "pump–probe" technique. Other

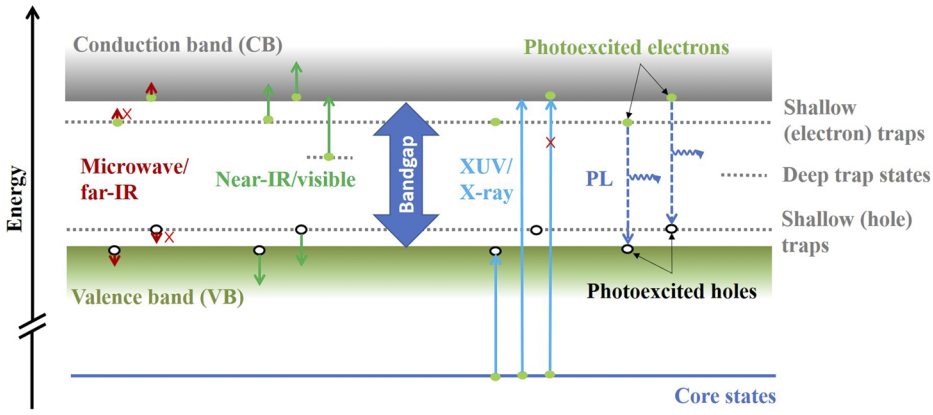

FIG. 1. Schematic flat-band representation of absorption (solid lines) of various wavelengths by and photoluminescence (PL, dashed lines) from an excited semiconductor photocatalyst. Green/hollow circles represent excited electrons/holes. Arrows labeled with a cross are forbidden transitions. For clarity, the trap states and core states have been collapsed and represented by single horizontal lines, but in general, these states have more than one energy level. For XUV/x-ray, a ground-state absorption is also shown for reference (middle blue arrow). Photoemission corresponds to the complete removal of an electron upon photon absorption and is not shown in this diagram.

pump–probe measurements including transient Raman[35] and photoemission techniques[36,37] have also been implemented. In general, note that most such time-resolved measurements have static equivalents routinely used for sample characterization. As such, the advantages and limitations of the time-resolved techniques are similar to those of its static counterparts.

Out of the techniques that use an electromagnetic probe to monitor the behavior of photoexcited species, probes in the visible and IR regions are most commonly used. The present review will focus on the application of pump–probe techniques that use visible/near-IR probes, which will be referred to as TAS (Transient Absorption Spectroscopy) from hereon. First, the background of TAS will be introduced in Sec. II; then, the ways in which TAS spectra can be obtained and interpreted will be discussed in Sec. III, followed by a discussion of ways in which TAS kinetics can be interpreted in Sec. IV. The application of TAS to photocatalysis, including its drawbacks, will be discussed along with an outlook of the technology in Sec. V.

II. INTRODUCTORY PRINCIPLES OF TRANSIENT ABSORPTION SPECTROSCOPY (TAS)

To some extent, TAS is essentially time-resolved UV–Vis, and absorbance can be obtained in either transmittance or reflectance geometries. Absorbance is a useful quantity because it is directly proportional to concentration (Beer–Lambert law), provided that the concentration of the species of interest is low enough that they do not significantly interact with one another. This assumption is applicable to many photocatalyst systems as the concentration of photogenerated charge carriers is generally quite low. However, the extinction coefficient of photoexcited charges is dependent on factors including sample porosity;[38] therefore, calculation of absolute electron/hole concentrations cannot be generally performed directly using extinction coefficients reported in the literature. TA signals are usually directly reported as changes in the absorbance or optical density (OD) of a material (the absorbance of a substance is also known as its optical density[39]).

Whereas stationary-state UV–Vis measures the ground-state sample, both ground state and excited states are measuredin TAS, and the transient absorption signal (ΔA) is defined as the difference between the absorbance of the excited and ground-state samples,

$$\Delta A(\lambda, \tau) = A^*(\lambda, \tau) - A^0(\lambda), \tag{1}$$

where $A^*(\lambda, \tau)$ and $A^0(\lambda)$, respectively, represent the absorbance of the excited and ground-state samples. The parameters λ (wavelength) and τ (time-delay) have been explicitly stated to emphasize that the transient signal is a function of both the (probe) wavelength and the pump–probe time-delay, defined as time elapsed after excitation.

In an experiment, the measurable quantity is the intensity of probe light transmitted or scattered by the sample. In transmission measurements, ΔA can be expressed in terms of measurable intensities as

$$\Delta A = \log\left(\frac{I}{I^*}\right), \tag{2}$$

where I and I^*, respectively, represent the intensities transmitted by the ground-state and excited samples. The way in which the sample is measured in transmission-mode TAS is illustrated in Fig. 2.

Broadly speaking, there are three electronic contributions to the TA signal: excited-state absorption [positive; excited-state absorption is sometimes referred to as Photo-Induced Absorption (PIA), but the former terminology will be used in the present work], stimulated emission (negative), and ground-state bleach (negative). The final observed TA signal is a sum of all three contributions.[13] The origin of these three contributions in the context of a semiconductor is schematically illustrated in Fig. 3. The form of contribution expected from the ground-state bleach can be inferred from the steady-state UV–Vis absorbance of a sample, whilst the form of contribution expected from stimulated emission can be inferred from the steady-state photoluminescence spectra. Apart from these electronic contributions, recently, the importance of contribution from thermal effects has also been emphasized,[40] which will be further discussed in Sec. III.

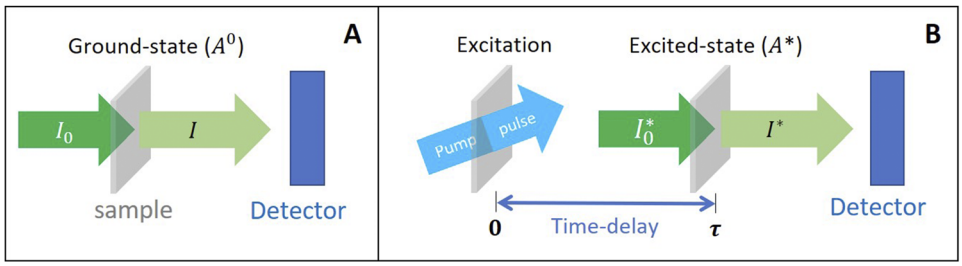

FIG. 2. Schematic illustrating the basic principle behind transmission-mode transient absorption spectroscopy, with panels (a) and (b), respectively, showing measurements of the sample in its ground and excited states. Panel (b) also illustrates that time-zero of the experiment is defined as the moment of sample excitation, and the time difference between the pump and probe pulses defines the time-delay (τ), which is varied to achieve time-resolution. I_0 and I, respectively, represent the incident and transmitted probe intensities through the ground-state sample, whilst I_0^* and I^*, respectively, represent the incident and transmitted intensities through the excited sample. In the ideal case, $I_0 = I_0^*$.

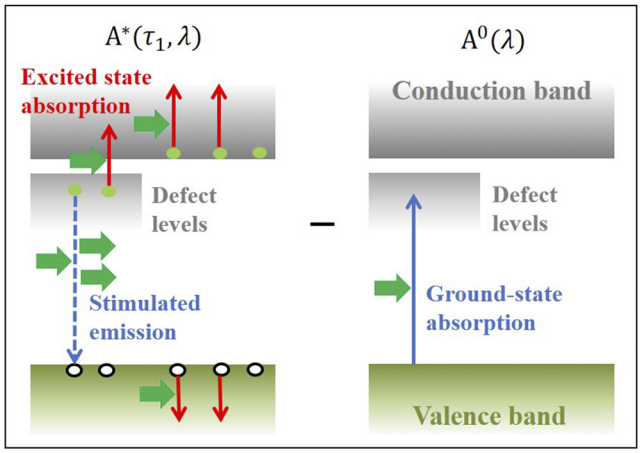

FIG. 3. Schematic illustrating the origins of excited-state absorption, stimulated emission, and ground-state bleach in the TA signal of a semiconductor. The ground-state absorption is always subtracted as a reference, so any absorption of the ground-state sample contributes as negative ground-state bleach in the final signal. Probe photons are shown as green arrows. Photoexcited electrons and holes are, respectively, shown as green and hollow circles.

III. TRANSIENT ABSORPTION SPECTRA

The final observed TA spectrum can be generally regarded as having contributions from all three electronic factors. In negative regions of the TA spectrum, it may be deduced that ground-state bleach and/or stimulated emission dominates over contributions from excited-state absorption, and vice versa for positive regions of the spectrum. In semiconductor systems, ground-state bleach can be expected to dominate the TA signal at probe energies above the bandgap. As the behavior of photoexcited charges is often the subject of interest, contributions to the TA signal from ground-state bleach and stimulated emission are often unwanted factors that complicate the analysis of TA data. In addition to this, recently, the importance of contribution from thermal effects to ultrafast TA spectra has been increasingly highlighted.[40] Contributions from the three aforementioned factors can be identified as being electronic in origin, which is distinct from thermal contributions. This section will begin with discussions that do not take thermal contributions into account; then, thermal contributions to TA spectra will be discussed toward the end of this section.

In general, it is difficult to break down a TA spectrum into contributions from excited-state absorption, stimulated emission, and ground-state bleach as it is not possible to measure each contribution accurately and separately. However, when it is reasonable to assume little contribution from stimulated emission and ground-state bleach, it is sometimes possible to identify contributions from different types of charge carriers (i.e., free/trapped electrons in/near the conduction band and holes in/near the valence band). One common method of distinguishing between electron and hole contributions to a transient absorption spectrum is to record the spectra in the presence of electron and hole scavengers. These scavengers capture photoexcited electrons/holes in the photocatalyst, thus, suppressing recombination, allowing long-lived counterparts to be observed. Depending on the nature of the scavenger used, the TA spectrum can be accordingly assigned. Apart from chemical scavengers,[18] electrical bias can also be used to assign spectral features in TA spectra.[5] Positive bias creates "excess" holes; therefore, the TAS signal of photoexcited holes can be identified. Similarly, negative bias creates "excess" electrons, therefore, allowing electron signals to be identified.

There are many studies reporting TAS on different semiconductors, and widely investigated materials include TiO_2,[17,41,42] WO_3,[43–45] C_3N_4,[46–48] and hematite.[49–51] Among these materials, TiO_2 and hematite are two typical examples. TiO_2 is the first material to be investigated by TAS, and hematite is the one most recently studied due to its favorable visible absorption and good stability. Therefore, subsequent discussions exemplifying the assignment of TA spectra will use hematite as the exemplar material.

Huang *et al.* made assignments to the TA spectrum of hematite films using difference spectra obtained through subtracting the spectrum of the biased hematite photoanode from the spectrum of the photoanode under open circuit conditions (no bias).[49] The TA spectrum 1 ns after photoexcitation and the difference spectra obtained at different biases are reproduced here in Fig. 4(a). The difference spectrum obtained at −1 V (vs Ag/AgCl) does not have any features that distinctly match the TA spectral features. However, the difference spectrum obtained at positive bias ("excess" holes) exhibited a sharp peak at 570 nm; the corresponding TA feature was, thus, accordingly attributed to hole absorption.[49] Interestingly, Huang *et al.* noted that the TA features do not change significantly with an applied external bias, the solvent environment (e.g., air, water, and methanol), or the sample morphology (films of different thickness, nanoparticle films, and colloidal particle suspensions). This is in stark contrast to work by Fitzmorris *et al.*, which found that TA spectra are qualitatively different between different nanostructured hematite samples,[50] but consistent with observations by Pendlebury *et al.* that the decay kinetics of photogenerated holes (monitored with 580 nm probe) in hematite films seem insensitive to the chemical environment.[51] Whereas Huang *et al.* attributed the insensitivity of TA features to various chemical parameters to the intrinsic origin of the TA features,[49] Pendlebury *et al.* attributed it to the short lifetime of holes in hematite in the absence of an external bias.[51] It is worth mentioning that Pendlebury *et al.* used a combination of electrical bias and chemical scavenger methods to assign the positive TA feature around 580 nm to surface active holes.[51] Under −0.1 V bias (vs Ag/AgCl), the TA kinetics monitored at 580 nm occur over the microsecond time scale, similar to those observed for isolated films. Upon the application of +0.4 V bias, the lifetime of the decay was extended to 3 s. When methanol was added, the lifetime under +0.4 V bias was reduced to 400 ms. These observations were used as evidence that the TA feature at 580 nm corresponds to surface active holes.[51]

The distinctive peak between 550 nm and 600 nm in the TA spectra of hematite was also observed by Barroso *et al.*, who assigned the feature to surface-trapped holes in the form of Fe^{4+},[52] based on that Fe^{4+} has been suggested to be responsible for absorption around 2.1 eV (~590 nm) in Fe-doped perovskites and TiO_2.[53,54] Later, Barroso *et al.* noted a sharp positive band at 580 nm in the difference spectra of hematite with and without (positive) bias, observed a corresponding feature in the TA spectra, and attributed it to holes in intra-bandgap states a few hundred millivolts below the conduction band.[55]

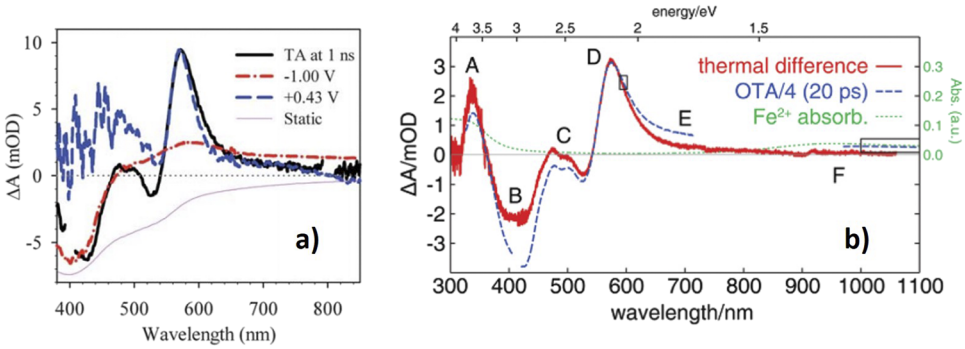

FIG. 4. Spectra reproduced from (a) Ref. 49 and (b) Ref. 59. Panel (a) compares the TA spectrum obtained 1 ns after 400 nm excitation of a hematite film in air (black line) with the steady-state difference spectrum obtained at −1 V and +0.43 V (vs Ag/AgCl) biases (red and blue lines, respectively). Inverted steady-state UV–Vis absorption is also shown in light pink. Panel (b) compares the TA spectrum of hematite obtained 20 ps after 415 nm excitation (blue line) with a steady-state difference spectrum between spectra taken at 500 K and 300 K (red line) and an absorption spectrum of $[Fe(H_2O)_6]^{2+}$ (green line).

It may be observed from above discussions that a sharp positive peak between 550 nm and 600 nm in the TA spectra of hematite is repeatedly assigned to the absorption of photoexcited holes. However, this positive peak is not always observed,[50,56] and alternative assignments of the peak exist. For example, Joly *et al.* observed a (broad) positive peak between 550 nm and 600 nm in the TA spectrum of hematite 300 fs after photoexcitation, but noted that this feature is very close to the bandgap, and, thus, attributed it to the bandgap shrinkage as hot electrons relax to the conduction band edge,[57] in accordance with theoretical calculations.[58] More recently, Hayes *et al.* provided strong evidence that the previously observed TA feature between 550 nm and 600 nm is thermal rather than electronic in origin.[59] Hayes *et al.* compared their TA spectrum of hematite with the thermal difference spectrum (obtained through subtracting the steady-state spectra at 500 K and 300 K) and found strong similarities between the two spectra,[59] reproduced here in Fig. 4(b). It was, thus, concluded that thermal contributions in the form of lattice expansion and thermal disorder, both of which can narrow the bandgap, dominate the TA spectrum of hematite.[59] In addition, it was found that as the excitation energy increased from 0.75 mJ cm^{-2} to 5.7 mJ cm^{-2}, the positive peak around 575 nm slightly shifted toward longer wavelengths,[59] which further supports its assignment to thermal effects. The disparity between TA and thermal difference spectra toward shorter wavelengths (<550 nm) was attributed to contributions from ground-state bleach and stimulated emission in TAS, while the disparity toward longer wavelengths (>600 nm) was proposed to be due to the difference between steady-state and ultrafast heating.[59] The decay kinetics monitored at 595 nm and 1050 nm were found to correlate well with one another, indicative of similar processes dominating the decay kinetics in these two wavelength regions. The only TA feature that Hayes *et al.* assigned to excited-state absorption was a band around 675 nm that almost completely decays within 100 ps.[59]

It seems that the assignment made by Hayes *et al.*[59] is in contradiction with assignments made by previously discussed works for the peak around 580 nm in the TA spectrum of hematite.[49,51,52] However, the various assignments can be reconciled when considering that distortions in the hematite lattice can also be induced by photoexcited charge carriers in the form of polarons. It is speculated here that the peak around 580 nm could be due to hole polarons associated with Fe^{4+} species, which could be generated either through heat, electrical bias, or photoexcitation. As holes are consumed through recombination, the distorted lattice also gradually returns to its ground-state form. Furthermore, in the absence of chemical scavengers, the decay of photoexcited holes is expected to correlate with the decay of electrons, and free charge carriers are expected to have increasing contribution toward longer wavelengths.[42,60] As such, the kinetics observed by Hayes *et al.*[59] at 1050 nm could well be due to recombination of electrons with holes. In summary, it is speculated here that the decays of photogenerated electrons and holes are both correlated with the relaxation of the distorted hematite lattice back to its ground state, which is responsible for the repeatedly observed positive TA peak between 550 nm and 600 nm for hematite. This assignment also explains the previously noted insensitivity of this peak to the chemical environment.

It is worth noting that the literature that takes thermal effects into account for analysis of TA data is not limited to those presented above for hematite,[60–63] and entanglement of contributions from thermal effects and electronic factors in various experiments has been known to be difficult to untangle for decades.[64–66] Overall, it has been highlighted that interpretation of TA spectra is generally not straightforward, and thermal effects, although often neglected, need to be considered. Extra caution must be taken when assigning TA signals near and above the bandgap of a material. Thermal effects that manifest as lattice expansions result in a slight bandgap reduction.[59,63] This shifts the absorption edge to longer wavelengths, which shows up in difference spectra as a distinct positive peak near the bandgap, as illustrated in Fig. 5.

Although above discussions have focused on hematite, as mentioned above, TAS spectra of other photocatalytic materials have also been extensively studied. Notably, the TA spectrum of various forms of TiO_2 has been repeatedly obtained using the chemical scavenger method by numerous literature studies spanning over several decades in time. For example, for the benchmark material anatase TiO_2, broad peaks around 400–500 nm and >650 nm are

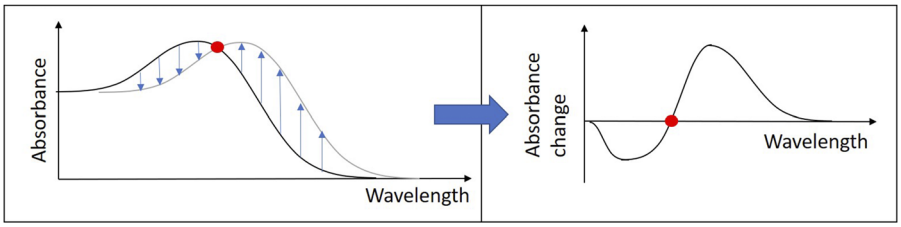

FIG. 5. Schematic illustrating how a red-shifted bandgap in the excited state results in a positive peak when taking the difference between the absorbance of the excited and ground states. The red circle marks the point where the absorbance change is zero.

commonly attributed to trapped holes and electrons, respectively.[17,42,67] Similarly, using chemical scavenger methods, TAS signals observed for WO_3 at probe wavelengths >750 nm have been attributed to photoexcited electrons and a peak around 475 nm to photoexcited holes.[43] In contrast, for the polymer photocatalyst graphitic carbon nitride, positive TAS signals spanning the entire visible and near-IR regions have been attributed to be primarily due to photoexcited electrons.[46] Note here that spectra reported for the same material can significantly differ from literature to literature. It has been previously noted that TA spectra can be very sensitive to conditions such as pH, surface conditions, and properties such as particle size.[17,42] The effect of parameters such as particle shape on the form of TA spectra can be exemplified by a piece of work by Fitzmorris *et al.*, who studied the TA features of four different nanostructured hematite and found the TA spectra to be qualitatively different between the different nanostructured samples.[50] In addition, Ruan *et al.* reported significantly different TA spectra for graphitic carbon nitride (g-CN) prepared through different methods.[47] In addition, experimental parameters such as excitation wavelength may also contribute to some apparent discrepancies between different works.

IV. TRANSIENT ABSORPTION KINETICS

In photocatalysis, the kinetic curves obtained with TAS are often compared between different samples. In many cases, slower TA decay kinetics are taken to represent slower electron–hole recombination, which usually translates into higher photocatalytic activity.[7,8,68] However, this is not always the case. For example, Dillon *et al.* observed the TA kinetics of four Au@TiO_2 core–shell nanostructures with different TiO_2 crystallinity and found the TA kinetic curves to overlap well with one another up to the longest time-delay of 1.5 ns, despite significant differences in the H_2-evolution capabilities of the samples.[69] This might be because charge carriers with lifetimes significantly longer than 1.5 ns are principally responsible for photocatalytic H_2-evolution and were not observed in the 1.5 ns experimental time-window for TAS. Thus, this section will introduce the three most commonly used equations for fitting TA kinetic data, followed by a discussion of example literature usage and interpretations.

The three most commonly used forms of equations for fitting kinetic TA data are (multi-)exponential, stretched exponential, and power-law decays. These are, respectively, of the forms

$$\Delta A(\tau) = \sum_i a_i e^{-\tau/\tau_i}, \tag{3}$$

$$\Delta A(\tau) = \sum_i a_i e^{-(\tau/\tau_i)^{\beta_i}}, \tag{4}$$

and

$$\Delta A(\tau) = a\tau^{-b}, \tag{5}$$

where $\Delta A(\tau)$ represents the TA signal at a specified probe wavelength, a_i and τ_i, respectively, represent the amplitude and lifetime of the ith contribution to the overall decay kinetics, β_i (>0 and <1) represents the ith stretching exponent, and b (>0) is the power-law exponent. These parameters are obtained through fitting experimental data.

Simple exponential decays are well-known to be characteristic of first-order kinetics,

$$\frac{dc}{dt} = -k_{1st}c, \tag{6}$$

where c represents the concentration of the reactant and k_{1st} represents the first-order rate constant. Integrating Eq. (6) for concentration varying from c_0 at time $t = 0$ to concentration c at time $t = \tau$ yields

$$c = c_0\, e^{-k_{1st}\tau}. \tag{7}$$

Extrapolating Eq. (7) to cases where several independent first-order reactions occur at the same time gives

$$\sum_i c(i) = \sum_i c_0(i) e^{-k_{1st}(i)\tau}. \tag{8}$$

In the context of TAS, $c(i)$ represents the concentration of the ith photoexcited species at time $t = \tau$ after excitation, $c_0(i)$ represents the initial concentration of the ith photoexcited species upon photoexcitation, and $k_{1st}(i)$ represents the first-order rate constant associated with the ith species. Following from discussions in Sec. II, $\Delta A(\tau)$ is directly proportional to the concentration of photoexcited species. As such, comparing Eq. (8) with Eq. (3) identifies $\Delta A(\tau) \propto \sum_i c(i)$, $a_i \propto c_0(i)$, and $\tau_i = 1/k_{1st}(i)$.

When Eq. (3) is used to fit TA kinetic curves, usually two or three terms are found to provide a good fit.[50,63,70,71] Although sometimes more terms are needed to fit a dataset,[49] the meaning of individual contributions becomes less clear. Generally, the more terms that are included in a fit, the better the fit, but the form of equation used cease to correspond to identifiable physical processes consuming photoexcited species. Sometimes, a constant offset is also found to be necessary to fit the data.[63,72] Fitting a constant offset either implies that the sample never relaxes back to its ground state (i.e., an irreversible change was induced upon photoexcitation) or that there is a decay component with time constant (τ_i) so long that $\tau_i \sim \infty$ in the context of time scales of the TAS experiment.

An implication of first-order kinetics is that the decay only depends on the concentration of a single species and, therefore,

cannot generally account for recombination of independent electrons and holes. The word independent is emphasized here, as excitons can be treated as a single entity (composed of an electron and a hole), and is, therefore, expected to decay according to first-order kinetics.

Alternatively, in a system composed of particles/crystallites, if the excitation intensity is low enough that on average only one electron–hole pair is generated per particle/crystallite, the TA kinetics are also expected to follow first-order rate laws, provided there is no interparticle/crystallite charge transfer. Generally, if primary geminate recombination is the dominant pathway through which charge carriers are consumed, first-order kinetics can be expected.

A well-known property of first-order kinetics is that the amount of time it takes for the concentration to reduce to half (defined as the half-life, $\tau_{1/2}$) is independent of initial concentration. Note here that $\tau_{1/2}$ (time taken for concentration to reduce to half its original value) is different from the lifetime (τ_i, time taken for concentration to reduce to e^{-1} its original value), but these terms are sometimes used synonymously in the literature.[73] In the context of TAS, first-order kinetics imply that kinetic curves recorded at different excitation intensities should overlap upon normalization of the decay curves. This is sometimes neglected in the literature. For example, Wang *et al.* studied the behavior of graphitic carbon nitride (g-CN) using femtosecond-TAS and found the observed kinetics to be well-fitted by a triple-exponential decay function.[74] Upon increasing the excitation intensity from 0.51 mJ/cm^2 to 0.85 mJ/cm^2, the three lifetimes were reduced from 3.5 ps to 3.3 ps, 60 ps to 26 ps, and 4.5 ns to 2.2 ns. The fastest component was assigned to intersystem crossing, the intermediate to triplet–triplet annihilation (generating a single–singlet exciton), and the slowest component to decay of singlet excitons.[74] Note here that (1) the three processes are not independent and, therefore, cannot be simply fit by the sum of three independent functions, (2) the decay kinetics are significantly accelerated upon increasing the excitation intensity, so the decay cannot be purely due to first-order processes, and (3) triplet–triplet annihilation is not a first-order process; thus, using an exponential function has little meaning in this case.

However, note here that true single-exponential kinetics have been observed in some cases. Cherepy *et al.* found that the TA kinetics observed for maghemite (γ-Fe_2O_3) nanoparticles over the picosecond-time scale are well-fitted to a triple-exponential function,[70] as illustrated by data reproduced here in Figs. 6(a) and 6(b). In addition, the decay kinetics over picosecond-time scales were found to be independent of excitation intensity,[70] as evident from data reproduced here in Fig. 6(c); it may be observed that the kinetics measured with 0.4 mJ/cm^2, 0.6 mJ/cm^2, and 1.2 mJ/cm^2 excitation intensities are well-overlapped with one another upon normalization.

The stretched-exponential decay could be equated to a linear combination of single-exponential functions with a continuous distribution of lifetimes and, therefore, can be taken to be a representative of a system possessing multiple relaxation pathways that exhibit single-exponential decay kinetics.[75,76] In this case, the parameters τ_i and β_i in Eq. (4), respectively, quantify the characteristic lifetime and the system heterogeneity, with $\beta = 1$ corresponding to a homogeneous system possessing a single relaxation pathway exhibiting first-order decay kinetics. However, when the stretched-exponential function is used to fit TA kinetics of photocatalysts, it is often used purely as a tool for quantifying the time constant without further interpretation of β.[18,69,77]

Alternative interpretations of stretched-exponential kinetics exist. Nelson *et al.* derived stretched-exponential behavior using a continuous-time random walk model for dye-sensitized TiO_2,

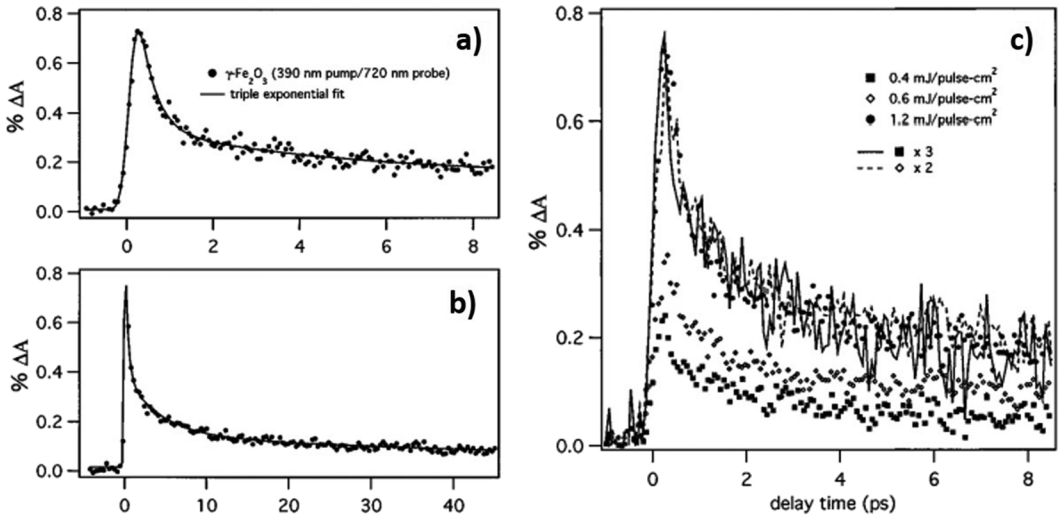

FIG. 6. TA kinetics of maghemite (γ-Fe_2O_3) monitored with 720 nm probe (a) up to 8.3 ps, (b) up to 48 ps after photoexcitation with 390 nm pump (1.2 mJ/cm^2), and (c) after photoexcitation with 390 pump of different intensities (0.4 mJ/cm^2, 0.6 mJ/cm^2, and 1.2 mJ/cm^2). In panels (a) and (b), the solid lines show the fitting function composed of triple-exponential decay convolved with a Gaussian. In panel (c), the solid and dashed lines also show the decay curves obtained after 0.4 mJ/cm^2 and 0.6 mJ/cm^2 excitation scaled by factors of 3 and 2, respectively. Reproduced from Ref. 70.

in which electron diffusion through a lattice occurs via multiple trap-detrapping from an exponential density of trap states into/out of the conduction band.[78] A stretched-exponential decay was predicted for dye cations in cases where electrons are in great excess compared to the cations. However, Barzykin *et al.* derived power-law kinetics for the long-time behavior of charge carriers assuming an exponential energetic distribution of trap states.[79] Many models have been developed for describing the behavior of photoexcited species,[79] but will not be further discussed here. In general, note that the non-exponential behavior is taken to be indicative of trap–detrap limited diffusion of charge carriers. In many cases, power-law kinetics are observed and attributed to the trap-detrapping limited recombination.[5,17,80,81] However, it is worth noting that stretched exponentials can be difficult to distinguish from power-law kinetics.

As expected for non-exponential kinetics, the decay kinetics are affected by the concentration of photogenerated charge carriers and, therefore, the excitation intensity, in contrast to exponential kinetics characteristic of first-order processes. For example, Tang *et al.* found that the TA kinetics of anatase TiO_2 in argon follow a power-law decay and are strongly intensity dependent, with the half-life of photoexcited charge carriers increasing as the excitation intensity decreases.[17] Intensity-dependence of decay kinetics has sometimes been taken to indicate second-order kinetics,[41,72,82] which is expected assuming a simple model for electron–hole recombination where electrons and holes diffuse around the photocatalyst in an analogous manner to two reactants in a solution. Under inert conditions, the concentration of photoexcited electrons is the same as the concentration of photoexcited holes, so the rate equation can be written as

$$\frac{dc}{dt} = -k_{2\mathrm{nd}}c^2, \tag{9}$$

where $k_{2\mathrm{nd}}$ is the second-order rate constant and c is the concentration of photoexcited electrons or holes. Integrating the above equation for electron/hole concentration varying from c_0 at time $t = 0$ to concentration c at time $t = \tau$ yields

$$c = \frac{c_0}{k_{2\mathrm{nd}}c_0\tau + 1}. \tag{10}$$

As previously mentioned, c is directly proportional to the transient absorption signal $\Delta A(\tau)$, so Eq. (10) can be written as

$$\Delta A(\tau) = \frac{pc_0}{k_{2\mathrm{nd}}c_0\tau + 1}, \tag{11}$$

where p is the constant of proportionality relating $\Delta A(\tau)$ to c. The above equation with a constant offset has been found to provide a good fit to TA kinetic data.

Both power-law decay and second-order kinetics can appear to be linear on a log–log plot. Taking the logarithm of Eq. (5) yields

$$\log(\Delta A(\tau)) = \log(a) - b * \log(\tau). \tag{12}$$

Therefore, a plot of log(ΔA(τ)) against log(τ) should yield a straight line with gradient −b. Similarly, taking the logarithm of Eq. (11) gives

$$\log(\Delta A(\tau)) = \log\left(\frac{p}{k_{2\mathrm{nd}}}\right) - \log\left(\tau + \frac{1}{k_{2\mathrm{nd}}c_0}\right). \tag{13}$$

As such, for sufficiently large $k_{2\mathrm{nd}}c_0$, a plot of log(ΔA(τ)) against log(τ) is also approximately a straight line, with gradient −1.

Following from above discussions, note here that for power-law decays, the exponent is sometimes found to be close to −0.5.[81] For this, a general consideration of a simple rate equation of the following form will be considered:

$$\frac{dc}{dt} = -kc^{\alpha}, \tag{14}$$

with α ≠ 1 and k representing a generic rate constant. Again, integrating the above equation for electron/hole concentration varying from c_0 at time $t = 0$ to concentration c at time $t = \tau$ yields

$$c = \left(\frac{{c_0}^{1-\alpha} - k\tau}{1-\alpha}\right)^{\frac{1}{1-\alpha}}. \tag{15}$$

Again, let p be the constant of proportionality relating $\Delta A(\tau)$ to c; then, following from Eq. (15),

$$\Delta A(\tau) = p\left(\frac{(1-\alpha)\,{c_0}^{1-\alpha} - k\tau}{1-\alpha}\right)^{\frac{1}{1-\alpha}}. \tag{16}$$

Substituting α = 2 into Eq. (16) yields Eq. (11). Taking the logarithm of Eq. (16) yields

$$\log(\Delta A(\tau)) = \frac{1}{1-\alpha}\left[\log\left(\tau - \frac{(1-\alpha)\,{c_0}^{1-\alpha}}{k}\right) + \log\left(\frac{k}{\alpha - 1}\right)\right] + \log(p). \tag{17}$$

Substituting α = 2 into the above equation yields Eq. (13). For sufficiently small $\frac{(1-\alpha)\,{c_0}^{1-\alpha}}{k}$, plots of log(ΔA(τ)) against log(τ) are approximately a straight line with gradient $\frac{1}{1-\alpha}$. For a slope of −0.5, α = 3. This could be taken to indicate the dominance of a 3-body process such as Auger recombination, which is feasible at high excitation intensities. Alternatively, trap-assisted recombination is effectively a 3-body process, because electron–hole recombination would depend on trap-state concentrations. However, usually linearity on a log–log plot is taken to be indicative of a power-law decay, with recombination limited by trap-detrapping of charge carriers.

In some cases, multiple processes may be consuming the same type of charge carrier in a photocatalyst. It is, thus, unsurprising that sometimes combinations of different functions are used to fit kinetic data to reflect this level of complexity. For example, Cowan *et al.* found that the TiO_2 photoelectrode held at 0 V in an alkaline solution exhibited TAS kinetics well-described by a linear combination of power-law and stretched-exponential decays, with the power-law dominating at early times (1–100 μs) and the stretched-exponential component dominating at later times.[5] The data and fit are reproduced here in Fig. 7(a). The power-law component was assigned to electron–hole recombination and the stretched-exponential component to the reaction between photogenerated holes and water. The magnitude of the electron–hole recombination component was

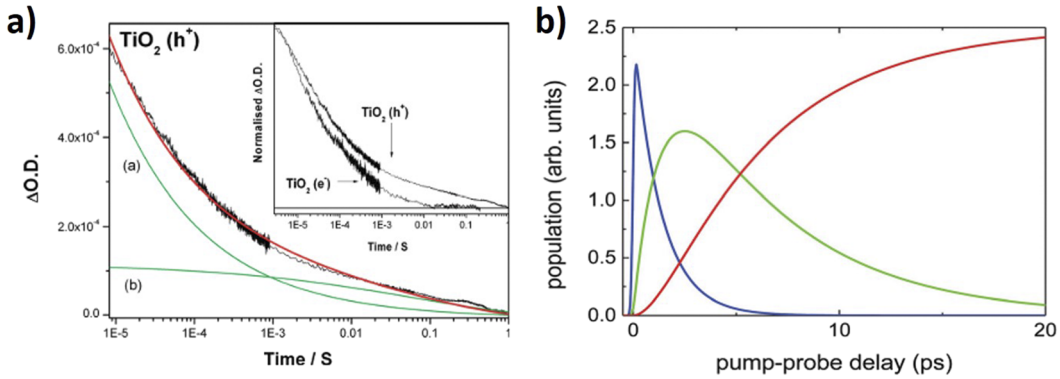

FIG. 7. TA kinetic data reproduced from (a) Ref. 5 and (b) Ref. 77. Panel (a) shows the TA kinetics monitored at 460 nm for the TiO_2 photoelectrode held at 0 V after 355 nm excitation (black line). The curve was fitted using a combination of power-law decay [green line, (a)] and stretched-exponential decay [green line, (b)]. The red line shows the overall fitted decay kinetics. The inset shows the normalized decay kinetics for electrons monitored at 800 nm probe wavelength and holes monitored at 460 nm, both recorded under the same conditions. Panel (b) shows the modeled time-evolution of excited charge carrier populations in WS_2 after photoexcitation, with the blue line representing the exciton population, and the green and red lines, respectively, representing the population of unbound and trapped charges. Non-exponential decay of the trapped charges is not observed over the displayed time scale.

found to be about 5 times larger than the photoreaction component 10 μs after photoexcitation, which was used to rationalize that the low quantum yield for O_2 production from water splitting is primarily due to fast electron–hole recombination.[5]

Rather than directly summing different contributions, Vega-Mayoral *et al.* analyzed the TA kinetics of WS_2 using a sequential model where the nature of charge carriers evolves as a function of time after photoexcitation.[77] The model assumes that excitons are the primary species generated upon photoexcitation, which exponentially decays into an intermediate state. The intermediate state then exponentially decays into final charges, which then relax non-exponentially to the ground state. The intermediate state and final charges were, respectively, identified as unbound and trapped charges. The dissociation of excitons into unbound charges was found to occur with a time constant of 1.3 ps, and the unbound charges become trapped with a time constant of 5.5 ps; then, the final trapped charges relax according to a stretched-exponential decay with a time constant of 450 ps and a stretching exponent of 0.3. The fitted curves for processes occurring over fast time scales (<20 ps) are produced here in Fig. 7(b). Note that in this cascade-like model, the overall population of excited charges is conserved until the last non-exponential step, and therefore, processes such as exciton–exciton annihilation are not accounted for.[77]

Note here that TAS studies outside heterogeneous photocatalysis often employ global and target analysis for extracting kinetic information from large datasets, in which kinetic data obtained at different probe wavelengths are collectively analyzed.[13,83,84] This type of analysis can also be potentially useful for extracting kinetic information about photocatalysts, as any one type of charge carrier can contribute to the TA signal at different probe wavelengths; therefore, certain kinetic components can be expected to be common across different wavelengths. However, global and target analysis is not commonly employed to analyze TAS data for heterogeneous photocatalysts, which could be because simple single-component (sometime double-component) analysis is often sufficient for purposes such as comparison of behavior of charge carriers in a photocatalyst under different chemical environments.

V. FURTHER DISCUSSIONS

Although long-lived charges are identified as a key requirement for photocatalytic activity to be observed,[8] long-lived charge carriers observed using TAS are not always useful for photocatalysis. Numerous literature studies have reported that graphitic carbon nitride (g-CN) samples that exhibit larger positive TA signals in the visible/near-IR region are less photocatalytically reductive, which is attributed to a higher concentration of inactive deep-trapped electrons that absorb visible light.[46,81,85] We suggested that for g-CN, excited electrons in shallow emissive states were in thermal equilibrium with electrons in deep non-emissive states.[46] The electrons in shallow emissive states have enough reductive potential for hydrogen production from water splitting, whilst the deep-trapped electrons that absorb in the visible region do not have enough reducing potential.[46] As such, although charge carriers observed by TAS are not always useful for photocatalysis, other understanding of the photocatalytic system may, nonetheless, be gained. As a further example, recently, we used TAS to rationalize the behavior of g-CN photoelectrodes.[47] It was found that the g-CN photoanode exhibits positive signals previously assigned to deep-trapped inactive electrons, whilst only negative TA signals were observed for the photocathode. It was, thus, concluded that there is a significant population of excited electrons in shallow emissive states that is responsible for the photocathode behavior, consistent with our previous model.[47]

VI. SUMMARY AND PERSPECTIVE

In this review, it has been demonstrated that Transient Absorption Spectroscopy (TAS) can be used to obtain useful information

to aid the understanding and continuous development of photocatalytic systems. The TA spectra of photoexcited electrons and holes can be identified using chemical scavengers or electrical bias. However, it has been increasingly highlighted recently that thermal effects can also contribute to the TA signal.[40] Common equations used to fit TA kinetics include single-exponential decay characteristic of first-order processes consuming photoexcited charge carriers, and stretched-exponential and power-law decays which can be interpreted as trap-detrapping limited recombination, although stretched-exponential decays can alternatively be interpreted as multiple first-order processes. Charge carrier recombination is sometimes modeled as a second-order process. In addition, it is speculated that gradients of −0.5 on a log–log plot could be indicative of 3-body processes consuming the population of photoexcited charge carriers.

In addition, it is interesting to note that the TA fingerprints of photoexcited holes are frequently reported to appear at 500–600 nm on different semiconductors, whilst the TA signatures of photoexcited electrons typically occur at longer wavelengths.[17,42–44] TAS is a very useful technique for characterizing the behavior of photoexcited charges in part due to the capability of this technique to measure several decades in time. However, it has been pointed out in the literature that TAS instrumentation usually either covers time ranges from tens of nanoseconds to milliseconds or from femtoseconds out to a maximum of a few nanoseconds, which often results in a time gap between achievable time ranges.[16] However, it is often informative to obtain a continuous kinetic trace from picoseconds to seconds. In the context of semiconductor photocatalysis, measuring from picosecond to second time scales would allow processes including charge generation, recombination, and interfacial charge transfer to be observed. Facilities exist that can cover the femtosecond to millisecond time range,[14,86] but often different instruments are used to cover the two different time ranges.[16,27,46]

It will also be noted here that TAS in combination with TRIR is a powerful combination of techniques, as TAS (with visible/near-IR probe) can monitor the behavior of deep-trapped charges, whilst TRIR is sensitive to free and shallow trapped charges. As previously mentioned, on some photocatalysts, deep-trapped charges are less photocatalytically active, while free and shallow trapped charges are expected to be the primary species facilitating photocatalysis. Charge carriers in different states have different contributions to the observed photocatalytic activity; therefore, obtaining information in both visible and IR regions is important. Furthermore, combining visible TAS with TRIR in the mid-IR region can potentially allow the mechanism of photocatalytic reactions to be elucidated. TAS allows the behavior of intrinsic charge carriers to be monitored, whilst TRIR can be used to monitor the vibrational changes associated with photocatalytic reactions taking place. Combining these techniques can, thus, allow the behavior of photoexcited charges to be correlated with the behavior of chemical species. However, one key problem is that excited charges often have large signals in the mid-IR region, which makes the kinetic signal from chemical species difficult to untangle from those due to photoexcited charges. This might be a reason for the apparent lack of studies that attempts to correlate the behavior of photoexcited charges monitored by TAS with chemical changes monitored by TRIR. In addition, monitoring molecular changes with TRIR is also intrinsically difficult due to factors such as small absorption coefficients associated with molecular vibrations.

ACKNOWLEDGMENTS

We are thankful for financial support from the RS International Exchanges 2017 Cost Share Award (Grant No. IEC\NSFC\170342), the UK EPSRC (Grant No. EP/N009533/1), the Royal Society-Newton Advanced Fellowship (Grant No. NA170422), and the Leverhulme Trust (Grant No. RPG-2017-122). Tina Jingyan Miao is also thankful for funding from the Molecular Modeling and Materials Science CDT (EPSRC) and the Central Laser Facility (STFC).

DATA AVAILABILITY

Data sharing is not applicable to this article as no new data were created or analyzed in this study.

REFERENCES

[1] C.-H. Liao, C.-W. Huang, and J. C. S. Wu, Catalysts **2**, 490 (2012).
[2] J. L. White, J. T. Herb, J. J. Kaczur, P. W. Majsztrik, and A. B. Bocarsly, J. CO2 Util. **7**, 1 (2014).
[3] G. P. Smestad and A. Steinfeld, Ind. Eng. Chem. Res. **51**, 11828 (2012).
[4] D. Das and T. Veziroglu, Int. J. Hydrogen Energy **33**, 6046 (2008).
[5] A. J. Cowan, J. Tang, W. Leng, J. R. Durrant, and D. R. Klug, J. Phys. Chem. C **114**, 4208 (2010).
[6] D. C. Hurum, A. G. Agrios, K. A. Gray, T. Rajh, and M. C. Thurnauer, J. Phys. Chem. B **107**, 4545 (2003).
[7] S. J. A. Moniz, S. A. Shevlin, D. J. Martin, Z.-X. Guo, and J. Tang, Energy Environ. Sci. **8**, 731 (2015).
[8] A. J. Cowan and J. R. Durrant, Chem. Soc. Rev. **42**, 2281 (2013).
[9] P. R. F. Barnes, K. Miettunen, X. Li, A. Y. Anderson, T. Bessho, M. Gratzel, and B. C. O'Regan, Adv. Mater. **25**, 1881 (2013).
[10] W. J. Youngblood, S.-H. A. Lee, K. Maeda, and T. E. Mallouk, Acc. Chem. Res. **42**, 1966 (2009).
[11] O. J. Sandberg, K. Tvingstedt, P. Meredith, and A. Armin, J. Phys. Chem. C **123**, 14261 (2019).
[12] L.-L. Li, Y.-C. Chang, H.-P. Wu, and E. W.-G. Diau, Int. Rev. Phys. Chem. **31**, 420 (2012).
[13] R. Berera, R. van Grondelle, and J. T. M. Kennis, Photosynth. Res. **101**, 105 (2009).
[14] E. C. Carroll, M. P. Hill, D. Madsen, K. R. Malley, and D. S. Larsen, Rev. Sci. Instrum. **80**, 026102 (2009).
[15] U. Schmidhammer, S. Roth, E. Riedle, A. A. Tishkov, and H. Mayr, Rev. Sci. Instrum. **76**, 093111 (2005).
[16] A. Yu, X. Ye, D. Ionascu, W. Cao, and P. M. Champion, Rev. Sci. Instrum. **76**, 114301 (2005).
[17] J. Tang, J. R. Durrant, and D. R. Klug, J. Am. Chem. Soc. **130**, 13885 (2008).
[18] J. Tang, A. J. Cowan, J. R. Durrant, and D. R. Klug, J. Phys. Chem. C **115**, 3143 (2011).
[19] J. B. Baxter and G. W. Guglietta, Anal. Chem. **83**, 4342 (2011).
[20] M. C. Beard, G. M. Turner, and C. A. Schmuttenmaer, J. Phys. Chem. B **106**, 7146 (2002).
[21] K. Shirai, T. Sugimoto, K. Watanabe, M. Haruta, H. Kurata, and Y. Matsumoto, Nano Lett. **16**, 1323 (2016).
[22] A. Yamakata, T.-a. Ishibashi, and H. Onishi, Bull. Chem. Soc. Jpn. **75**, 1019 (2002).
[23] K. Koike, D. C. Grills, Y. Tamaki, E. Fujita, K. Okubo, Y. Yamazaki, M. Saigo, T. Mukuta, K. Onda, and O. Ishitani, Chem. Sci. **9**, 2961 (2018).

[24]C. D. Windle, M. W. George, R. N. Perutz, P. A. Summers, X. Z. Sun, and A. C. Whitwood, Chem. Sci. **6**, 6847 (2015).
[25]A. Yamakata, T.-a. Ishibashi, and H. Onishi, J. Mol. Catal. A: Chem. **199**, 85 (2003).
[26]S. Shen, X. Wang, T. Chen, Z. Feng, and C. Li, J. Phys. Chem. C **118**, 12661 (2014).
[27]A. Yamakata, M. Kawaguchi, N. Nishimura, T. Minegishi, J. Kubota, and K. Domen, J. Phys. Chem. C **118**, 23897 (2014).
[28]A. Yamakata, H. Yeilin, M. Kawaguchi, T. Hisatomi, J. Kubota, Y. Sakata, and K. Domen, J. Photochem. Photobiol., A **313**, 168 (2015).
[29]J. Vura-Weis, C.-M. Jiang, C. Liu, H. Gao, J. M. Lucas, F. M. F. De Groot, P. Yang, A. P. Alivisatos, and S. R. Leone, J. Phys. Chem. Lett. **4**, 3667 (2013).
[30]S. Neppl, J. Mahl, A. S. Tremsin, B. Rude, R. Qiao, W. Yang, J. Guo, and O. Gessner, Faraday Discuss. **194**, 659 (2016).
[31]A. Cirri, J. Husek, S. Biswas, and L. R. Baker, J. Phys. Chem. C **121**, 15861 (2017).
[32]J. Liqiang, Q. Yichun, W. Baiqi, L. Shudan, J. Baojiang, Y. Libin, F. Wei, F. Honggang, and S. Jiazhong, Sol. Energy Mater. Sol. Cells **90**, 1773 (2006).
[33]M. Li, G. Xing, L. F. N. Ah Qune, G. Xing, T. Wu, C. H. A. Huan, X. Zhang, and T. C. Sum, Phys. Chem. Chem. Phys. **14**, 3075 (2012).
[34]W.-J. Ong, L. K. Putri, Y.-C. Tan, L.-L. Tan, N. Li, Y. H. Ng, X. Wen, and S.-P. Chai, Nano Res. **10**, 1673 (2017).
[35]S. K. Sahoo, S. Umapathy, and A. W. Parker, Appl. Spectrosc. **65**, 1087 (2011).
[36]R. Yukawa, S. Yamamoto, K. Ozawa, M. Emori, M. Ogawa, S. Yamamoto, K. Fujikawa, R. Hobara, S. Kitagawa, H. Daimon, H. Sakama, and I. Matsuda, Appl. Phys. Lett. **105**, 151602 (2014).
[37]S. Yamamoto and I. Matsuda, J. Phys. Soc. Jpn. **82**, 021003 (2013).
[38]A. J. Cowan, W. Leng, P. R. F. Barnes, D. R. Klug, and J. R. Durrant, Phys. Chem. Chem. Phys. **15**, 8772 (2013).
[39]C. Schaschke, *A Dictionary of Chemical Engineering* (Oxford University Press, 2014).
[40]K. E. Knowles, M. D. Koch, and J. L. Shelton, J. Mater. Chem. C **6**, 11853 (2018).
[41]D. P. Colombo and R. M. Bowman, J. Phys. Chem. **99**, 11752 (1995).
[42]T. Yoshihara, R. Katoh, A. Furube, Y. Tamaki, M. Murai, K. Hara, S. Murata, H. Arakawa, and M. Tachiya, J. Phys. Chem. B **108**, 3817 (2004).
[43]F. M. Tachiya, A. J. Cowan, B. D. Alexander, J. R. Durrant, and D. R. Klug, J. Phys. Chem. Lett. **2**, 1900 (2011).
[44]V. Cristino, S. Marinello, A. Molinari, S. Caramori, S. Carli, R. Boaretto, R. Argazzi, L. Meda, and C. A. Bignozzi, J. Mater. Chem. A **4**, 2995 (2016).
[45]I. Bedja, S. Hotchandani, and P. V. Kamat, J. Phys. Chem. **97**, 11064 (1993).
[46]R. Godin, Y. Wang, M. A. Zwijnenburg, J. Tang, and J. R. Durrant, J. Am. Chem. Soc. **139**, 5216 (2017).
[47]Q. Ruan, T. Miao, H. Wang, and J. Tang, J. Am. Chem. Soc. **142**, 2795 (2020).
[48]H. Zhang, Y. Chen, R. Lu, R. Li, and A. Yu, Phys. Chem. Chem. Phys. **18**, 14904 (2016).
[49]Z. Huang, Y. Lin, X. Xiang, W. Rodríguez-Córdoba, K. J. McDonald, K. S. Hagen, K.-S. Choi, B. S. Brunschwig, D. G. Musaev, C. L. Hill, D. Wang, and T. Lian, Energy Environ. Sci. **5**, 8923 (2012).
[50]B. C. Fitzmorris, J. M. Patete, J. Smith, X. Mascorro, S. Adams, S. S. Wong, and J. Z. Zhang, ChemSusChem **6**, 1907 (2013).
[51]S. R. Pendlebury, M. Barroso, A. J. Cowan, K. Sivula, J. Tang, M. Grätzel, D. Klug, and J. R. Durrant, Chem. Commun. **47**, 716 (2011).
[52]M. Barroso, A. J. Cowan, S. R. Pendlebury, M. Grätzel, D. R. Klug, and J. R. Durrant, J. Am. Chem. Soc. **133**, 14868 (2011).
[53]B. W. Faughnan and Z. J. Kiss, Phys. Rev. Lett. **21**, 1331 (1968).
[54]A. J. Nozik, J. Phys. C: Solid State Phys. **5**, 3147 (1972).
[55]M. Barroso, C. A. Mesa, S. R. Pendlebury, A. J. Cowan, T. Hisatomi, K. Sivula, M. Gratzel, D. R. Klug, and J. R. Durrant, Proc. Natl. Acad. Sci. U. S. A. **109**, 15640 (2012).
[56]L. Fu, Z. Wu, X. Ai, J. Zhang, Y. Nie, S. Xie, G. Yang, and B. Zou, J. Chem. Phys. **120**, 3406 (2004).
[57]A. G. Joly, J. R. Williams, S. A. Chambers, G. Xiong, W. P. Hess, and D. M. Laman, J. Appl. Phys. **99**, 053521 (2006).
[58]B. R. Bennett, R. A. Soref, and J. A. Del Alamo, IEEE J. Quantum Electron. **26**, 113 (1990).
[59]D. Hayes, R. G. Hadt, J. D. Emery, A. A. Cordones, A. B. F. Martinson, M. L. Shelby, K. A. Fransted, P. D. Dahlberg, J. Hong, X. Zhang, Q. Kong, R. W. Schoenlein, and L. X. Chen, Energy Environ. Sci. **9**, 3754 (2016).
[60]J. K. Cooper, S. E. Reyes-Lillo, L. H. Hess, C.-M. Jiang, J. B. Neaton, and I. D. Sharp, J. Phys. Chem. C **122**, 20642 (2018).
[61]A. J. Sabbah and D. M. Riffe, Phys. Rev. B **66**, 165217 (2002).
[62]Y. M. Sheu, S. A. Trugman, Y.-S. Park, S. Lee, H. T. Yi, S.-W. Cheong, Q. X. Jia, A. J. Taylor, and R. P. Prasankumar, Appl. Phys. Lett. **100**, 242904 (2012).
[63]S. Y. Smolin, A. K. Choquette, J. Wang, S. J. May, and J. B. Baxter, J. Phys. Chem. C **122**, 115 (2018).
[64]M. Terazima and N. Hirota, J. Phys. Chem. **96**, 7147 (1992).
[65]M. Terazima, T. Hara, and N. Hirota, J. Phys. Chem. **97**, 13668 (1993).
[66]M. Terazima, T. Hara, and N. Hirota, J. Phys. Chem. **97**, 10554 (1993).
[67]D. Bahnemann, A. Henglein, and L. Spanhel, Faraday Discuss. Chem. Soc. **78**, 151 (1984).
[68]M. Lan, G. Fan, L. Yang, and F. Li, RSC Adv. **5**, 5725 (2015).
[69]R. J. Dillon, J.-B. Joo, F. Zaera, Y. Yin, and C. J. Bardeen, Phys. Chem. Chem. Phys. **15**, 1488 (2013).
[70]N. J. Cherepy, D. B. Liston, J. A. Lovejoy, H. Deng, and J. Z. Zhang, J. Phys. Chem. B **102**, 770 (1998).
[71]H. M. Fan, G. J. You, Y. Li, Z. Zheng, H. R. Tan, Z. X. Shen, S. H. Tang, and Y. P. Feng, J. Phys. Chem. C **113**, 9928 (2009).
[72]A. Furube, T. Shiozawa, A. Ishikawa, A. Wada, K. Domen, and C. Hirose, J. Phys. Chem. B **106**, 3065 (2002).
[73]S. R. Pendlebury, A. J. Cowan, M. Barroso, K. Sivula, J. Ye, M. Grätzel, D. R. Klug, J. Tang, and J. R. Durrant, Energy Environ. Sci. **5**, 6304 (2012).
[74]H. Wang, S. Jiang, S. Chen, X. Zhang, W. Shao, X. Sun, Z. Zhao, Q. Zhang, Y. Luo, and Y. Xie, Chem. Sci. **8**, 4087 (2017).
[75]K. C. B. Lee, J. Siegel, S. E. D. Webb, S. Lévêque-Fort, M. J. Cole, R. Jones, K. Dowling, M. J. Lever, and P. M. W. French, Biophys. J. **81**, 1265 (2001).
[76]D. C. Johnston, Phys. Rev. B **74**, 184430 (2006).
[77]V. Vega-Mayoral, D. Vella, T. Borzda, M. Prijatelj, I. Tempra, E. A. A. Pogna, S. Dal Conte, P. Topolovsek, N. Vujicic, G. Cerullo, D. Mihailovic, and C. Gadermaier, Nanoscale **8**, 5428 (2016).
[78]J. Nelson, S. Haque, D. Klug, and J. Durrant, Phys. Rev. B **63**, 205321 (2001).
[79]A. V. Barzykin and M. Tachiya, J. Phys. Chem. B **106**, 4356 (2002).
[80]Y. Yamada and Y. Kanemitsu, Appl. Phys. Lett. **101**, 133907 (2012).
[81]J. J. Walsh, C. Jiang, J. Tang, and A. J. Cowan, Phys. Chem. Chem. Phys. **18**, 24825 (2016).
[82]A. Furube, T. Asahi, H. Masuhara, H. Yamashita, and M. Anpo, J. Phys. Chem. B **103**, 3120 (1999).
[83]I. H. M. Van Stokkum, D. S. Larsen, and R. Van Grondelle, Biochim. Biophys. Acta, Bioenerg. **1657**, 82 (2004).
[84]C. Slavov, H. Hartmann, and J. Wachtveitl, Anal. Chem. **87**, 2328 (2015).
[85]R. Kuriki, H. Matsunaga, T. Nakashima, K. Wada, A. Yamakata, O. Ishitani, and K. Maeda, J. Am. Chem. Soc. **138**, 5159 (2016).
[86]G. M. Greetham, D. Sole, I. P. Clark, A. W. Parker, M. R. Pollard, and M. Towrie, Rev. Sci. Instrum. **83**, 103107 (2012).